ChemComm

Accepted Manuscript

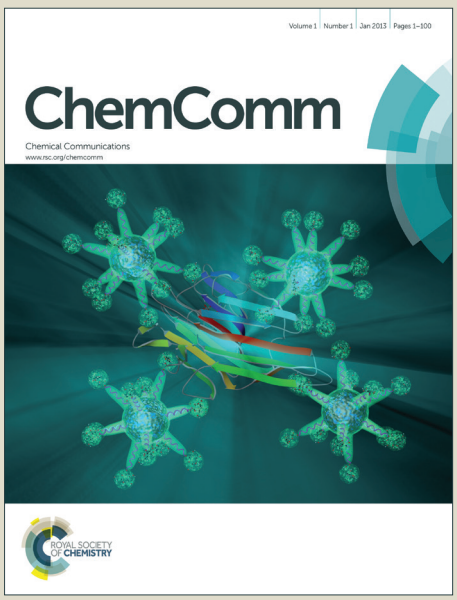

ROYAL SOCIETY OF CHEMISTRY

www.rsc.org/chemcomm

Journal Name

RSCPublishing

COMMUNICATION

Directed flexibility: self–assembly of a supramolecular tetrahedron

Cite this: DOI: 10.1039/x0xx00000x

James M. Ludlow III,[a] Tingzheng Xie,[a] Zaihong Guo,[b] Kai Guo,[a] Mary Jane Saunders,[d] Charles N. Moorefield,[c] Chrys Wesdemiotis,*[a,b] and George R. Newkome*[a,b]

Received 00th January 2012,
Accepted 00th January 2012

DOI: 10.1039/x0xx00000x

www.rsc.org/

Self-assembly of a tribenzo-27-crown-9 ether functionalized with six terpyridines generated (85 %) an expanded tetrahedral structure comprised of four independent triangular surfaces interlinked by crown ether vertices.

Metal–ligand self-assembly has been utilized to form various metallosupramolecular structures including coordination polymers,[1] macrocycles,[2-7] and 3D structures.[2,8] The *N*-heteroaromatic ligand [2,2':6',2"]terpyridine (tpy) has received increasing attention due in part to its ability to coordinate diverse transition metals permitting control of bond strengths, properties, and desired molecular architectures.[1,9] With metals that can form strong coordinative bonds, *e.g.* Os^{2+}, Ru^{2+}, and Fe^{2+}, the final product is kinetically determined by creating irreversible <tpy-M^{2+}-tpy> linkages; in contrast, metals capable of more labile coordinative bonds, *e.g.* Zn^{2+} and Cd^{2+}, give access to the thermodynamic products.

Specific architectures are determined, in part, by the geometry of the building blocks, *i.e.* angle(s) of the conjoined ligands with respect to one another. Exploiting the angular orientation and stoichiometric control of precursors is generally known as a directional bonding approach to supramolecular synthesis.[2] As shown in Scheme 1, ligands with 60° angles have been used to form triangular structures.[7,10] The structural and kinetic favorability of triangular-based systems has been harnessed, through use of multitopic 60°-based ligands to create large and intricate architectures, such as a spoked wheel[6] and the Sierpiński triangle.[11] A synthetic improvement *via* replacement of a 120° angle with two 60° angles has also been demonstrated.[12] These triangle-based architectures are planar and utilize 60° ligands, *e.g.* *ortho*-aryls, and can introduce a rigid framework into the resultant end product. Likewise, in biomolecular systems, directionality and positioning of non-covalent interactions are critical to molecular recognition and supramolecular structure formation, for example hydrogen bonding in protein structures and base pairing in DNA. Also, flexibility plays a key role in such systems to allow the folding and winding necessary to achieve the required structure and function. Using a similar strategy of balanced directionality and flexibility, Scheme 1 depicts the quantitative construction of a rigid triangular component[7] that can be used to align other highly flexible components, such as the tribenzo-27-crown-9 ethereal vertices (Schemes 2 and 3). Flexible linkages, such as crown ethers, have been used in conjunction with multitopic terpyridine ligands;[13] however, these examples did not incorporate angular directionality and isolation of cyclic species required use of non-labile metals and purification *via* chromatography. Flexibility can also be incorporated into cage forming *N*-donor ligands via methylene bridges[14,15] and polyester moieties.[16]

Herein, we describe the design and synthesis (Scheme 2) of a novel hexa*kis*terpyridine ligand containing three 60° juxtaposed *bis*ligands connected by a flexible crown ether vertex (**5**) and demonstrate its self-assembly with Zn^{2+} to generate an expanded tetrahedral structure under thermodynamic control (Scheme 3). The flexible vertex allows an extension into a 3D structure, which was studied *via* ESI-TWIM-MS, TEM, 1D and 2D NMR, as well as molecular modeling. The NMR studies and molecular modeling indicate the presence of parallel (π-π) and T-shaped (CH-π) interactions of stacked tpy complexes, which would be forbidden by more traditional, rigid architectures. A model 'free triangle' (**2**) is synthesized for comparison (Scheme 1) to demonstrate the influence of the tetrahedral structure.

Scheme 1. Synthesis of the simplest 'free triangle' **2**.

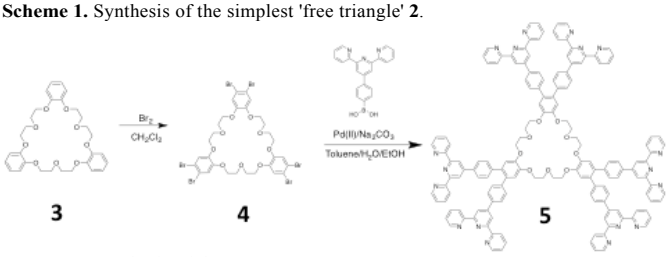

Scheme 2. Synthesis of the vertex reagent **5.**

Tribenzo-27-crown-9 (**3**), synthesized using a literature methods,[17] was brominated and then subjected to a Suzuki coupling[18] with 4-([2,2':6',2"]terpyridin-4'-yl)phenylboronic acid to give the desired ligand **5**, which was subsequently self-assembled with Zn^{2+} (Scheme 2) to give the desired tetrahedron **L4M12**.

The ^{1}H NMR of **L4M12** reveals a single set of terpyridine resonances indicative of a highly symmetrical structure. The spectrum is consistent with fully complexed cyclic structures that exhibit the expected upfield shifted 6,6"-tpy*H* signals (8.65 to 7.59 ppm, Figure

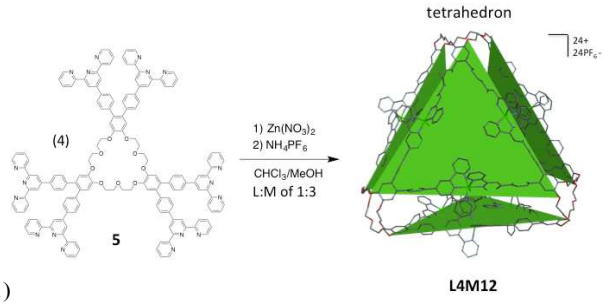

Scheme 3. Complexation of **5** to form **L4M12**. The structure's four independent triangles, each analogous to **2**, are highlighted in green to aid in visualization of the structure. **L4M12** is a combination of 4 ligands and 12 metals (Zn^{2+}).

thereby supporting the *bis*terpyridine Zn^{2+} complexation; no uncomplexed terpyridine was observed. Both COSY and NOESY ^{1}H NMR confirmed proton assignments (Figures S5-8 in the Supplemental Information).

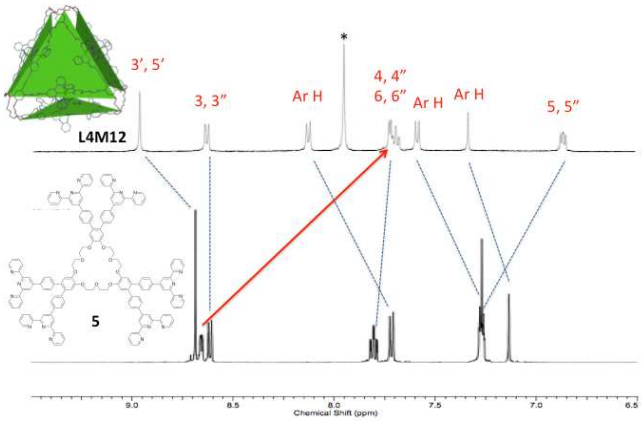

Figure 1. 500 MHz ^{1}H NMR spectra – aromatic region at 20 °C. Bottom: neat ligand **5** ($CDCl_3$) at 10 mg/mL and top: **L4M12** in CD_3CN/DMF-d_7.(5:1) at 0.6 mg/mL *-DMF.

Figure 2 compares the aromatic regions of **2** and **L4M12**. Since the 'free triangle' **2** is, essentially, chemically identical to the interlinked triangles of **L4M12**, any differences observed in chemical shift must arise from the **L4M12**'s supramolecular structure. A single set of terpyridines is observed for each, with the sole exception of the aryl singlets, all of the resonances of **L4M12** are shifted upfield, most notably the 4,4"-, 5,5"-, and 6,6"-tpy protons, suggesting that the tetrahedral structure has a significant shielding effect. Molecular modeling shows that the complexes of adjacent triangles are stacked; thus, the observed shielding effect is consistent with previously reported structures involving stacked <tpy-M^{2+}-tpy> complexes.[19,20]

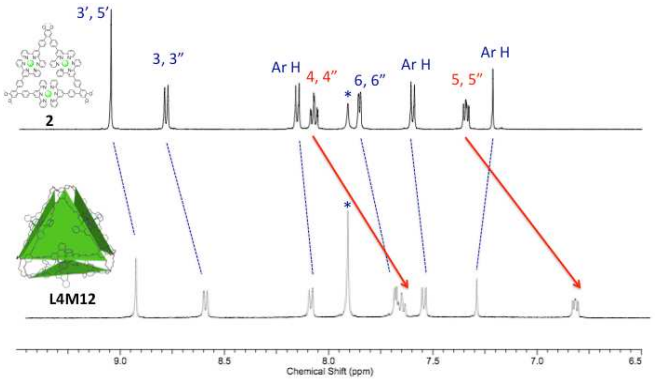

Figure 2. 500 MHz ^{1}H NMR of **2** (top, 3.0 mg/mL) and **L4M12** (bottom, 0.6 mg/mL) both in CD_3CN/DMF-d_7.(5:1) at 20 °C. *-DMF.

Variable temperature (VT) ^{1}H NMR experiments were conducted on both **L4M12** and **2**. As the temperature was lowered, the chemical shift attributed to the **L4M12** shows that the 5,5" peaks are shifted upfield. Conversely, the chemical shifts of the protons in **2** were insensitive to temperature variations (Figure S9). Similar chemical shift changes with temperature were also observed with stacked <tpy-M^{2+}-tpy> complexes.[19,20] This result implies that, as molecular motion is decreased, the shielding effect from the tetrahedral structure is enhanced. Conversely, the environment of the aromatic protons of **2**, where intramolecular stacking cannot occur, has been shown to be insensitive to the degree-of-molecular motion. Previous reports[21] indicate that the proton signals of cyclic <tpy-M^{2+}-tpy> trimers, such as **2,** show negligible chemical shift changes when the temperature is varied.

L4M12 was characterized by ESI–MS (Figure 3). The series of peaks match with charge states 5+ through 10+ for the combination of 4 ligands, 12 metals (Zn^{2+}), and the corresponding number of PF_6^- anions. ESI-MS coupled with travelling wave ion mobility[22] (TWIM) was used to further support the tetrahedral structure (Figure 4). **L4M12** shows the expected step pattern of charge states. Each charge state has a narrow drift time distribution indicative of an absence of superimposed isomers or conformers. Experimental collision cross-sections were calculated using the TWIM data and are shown in Table 1.[6,23-27]; the Collision Cross-Section (CCS) of an ion can be viewed as its apparent forward-moving surface area. Energy minimized structures were used to calculate a theoretical CCS for the counterion-free assembly using the Projection Approximation (PA), Trajectory Method (TM), and Exact Hard Sphere Scattering (EHSS) methods available in the MOBCAL program. The correlation between the theoretical and experimental values provides further support for the proposed architecture. Gradient tandem mass spectrometry[22] (gMS^2) was used to probe the stability of **L4M12** by subjecting the 10+, 8+, and 6+ charge states to collisionally activated dissociation (with Ar gas) prior to ion mobility separation (Figure S11). Collision energies of 45, 60, and 80 eV, respectively, were required to fully dissociate the complex. These translate into center-of-mass collision energies (E_{cm}) of 1.0184, 1.0614, and 1.0376 eV.

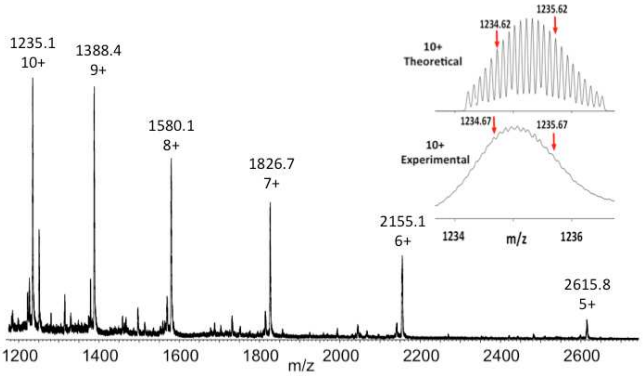

Figure 3. ESI-MS of **L4M12** showing a series of peaks corresponding to charge states 5+ thru 10+ and (inset) theoretical and experimental isotope patterns for the 10+ charge state; 0.6 mg/mL in MeCN/DMF (5:1).

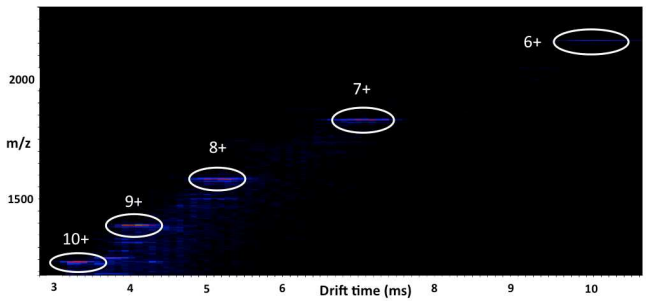

Figure 4. ESI-TWIM-MS plot of **L4M12** (*m/z vs*. drift time). 0.6 mg/mL in MeCN/DMF (5:1).

Z	$CCS_{exp}(Å^2)$	$CCS_{exp}(Å^2)$ Average	$CCS_{theo}(Å^2)$
6+	1351.6	1284.4(40.8)	1409(8)-EHSS
7+	1306.6		1385(19)-TM
8+	1278.9		1136(6)-PA
9+	1265.0		
10+	1219.7		

Table 1. Experimental and theoretical CCS values for **L4M12**. Standard deviations are in parenthesis.

A dilute solution of **L4M12** (*ca*. 10^{-5} M, MeCN/DMF, 5/1) was cast onto Cu grids and observed *via* transmission electron microscopy (TEM). Dimensions of the observed, discrete nanostructures (Figure 5) correspond well with measured molecular model dimensions. The calculated edge length for the tetrahedron is *ca*. 3.5 nm, which closely matches the *ca*. 4 nm. observed in the TEM. Molecular modeling of **L4M12** (Figure 5) also indicates close proximity of adjacent complexes. The <tpy-M^{2+}-tpy> protons are projected into the adjacent complex unit and should, therefore, be more highly shielded than in a non-stacked complex, such as the free triangle as is demonstrated in Figure 2. These results match with observations seen in previously reported stacked <tpy-M^{2+}-tpy> species.[13,19] The presence of the slipped parallel (π-π) and T-shaped (CH-π) stacking interactions are shown; these π-π interactions are generally regarded as energetically favorable, and are reported[28] to be -6.2 and -10.3 kJ-mol^{-1}, respectively, in model systems. Such cooperative interactions could stabilize the tetrahedral structure and/or promote its formation relative to other structures in which such intramolecular interactions do not occur. Metal-to-metal distances in the model closely match those reported[19] for stacked tpy complexes formed from parallel *bis*-ligands. For example, the metal-to-metal distances in **L4M12** ranged from *ca.* 9.2 to 9.5 Å *vs*. 8.8Å in the reported complex.[19] Stacked tpy complexes have been confirmed in a variety of solid-state structures[29].

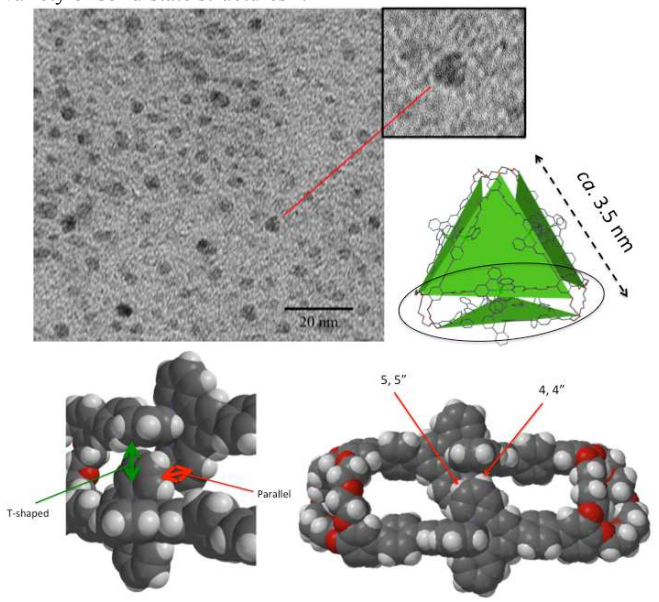

Figure 5. TEM with magnified inset and space filling model cutaways of **L4M12** showing stacked <tpy-M^{2+}-tpy> complexes. Color scheme: H: white; C: grey; N: purple; O: red; Zn: green. The 4,4" and 5,5" protons are noted (right). Regions of T-shaped (CH-π) and parallel (π-π) interactions are noted (left).

The internal volume of **L4M12** is estimated to be *ca.* 2400 Å^3, making it an excellent candidate for guest-host chemistry.[30] ^{19}F NMR was used to probe anion encapsulation properties of **L4M12** in solution. The ^{19}F spectra of **L4M12** with PF_6^- counterions (volume 62Å^3) only showed one peak. Previous studies[14] of cage-like structures using PF_6^- have reported that this occurs with rapid endo-exo anion exchange relative to the NMR timescale.[14,31] To reduce the exchange rate, the larger and tetrahedral anion, tetra*kis*(perfluorophenyl)borate (BARF) (volume 446 Å^3), was used to precipitate **L4M12**. The ^{19}F NMR of **L4M12** with BARF counterions showed the presence of additional, smaller peaks at -151.6, -182.7, and -183.8 ppm (Figure 6) suggesting the presence of a dynamic equilibrium of one or more BARF counterions within the cavity. As expected, these endo peaks were not detected with **2** using BARF as the counterions.

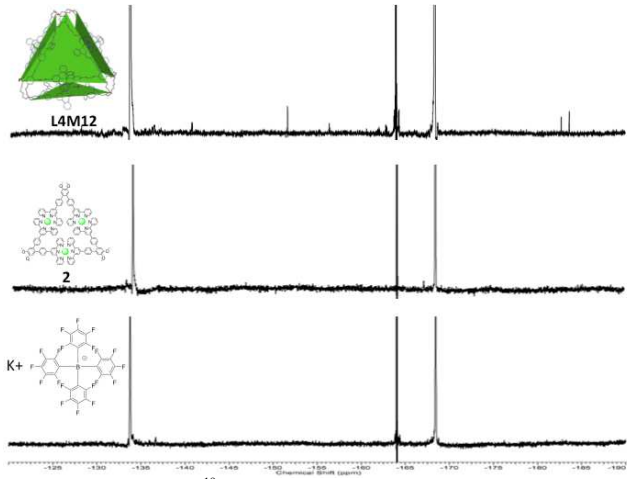

Figure 6. The 470MHz ^{19}F NMR of **L4M12** (top) and **2** (middle) both in $CD_3CN/DMF\text{-}d_7$.(5:1) at 20 °C, 1 mg/mL with BARF counterions. Bottom spectra shows neat K-tetra*kis*(perfluorophenyl)borate.

Finally, using a strategy of balanced directionality and flexibility, we describe the design and synthesis of a novel hexa*kis*terpyridine ligand containing a trio of 60°-directed *bis*ligands connected by crown ether vertices and its self-assembly into a tetrahedral structure under thermodynamic control. The flexible vertex allows a controlled extension into new 3D structures facilitated by intramolecular π-π interactions. Molecular modeling supports the NMR data suggesting the presence of parallel (π-π) and T-shaped (CH-π) interactions in the close-packed tpy complexes. VT NMR experiments support this model in which ^{19}F NMR experiments are indicative of the presence of BARF within the cavity. The crown ether groups can serve as "pores" or ports for molecular guests and/or anchoring sites for further supramolecular interactions; work in this direction is ongoing.

Acknowledgments

Support is acknowledged from the National Science Foundation (CHE-11-51991, GRN; CHE-1308307, CW) and The Ohio Board of Regents. We thank Benjamin Thome and Nicholas Johnson (UA) for valuable expertise and assistance with the VT NMR experiments.

Notes and references

Departments of [a]Polymer Science and [b]Chemistry, and [c]The Maurice Morton Institute for Polymer Science, The University of Akron, Akron, OH 44325-4717 USA. Tel: 330-972-6458; [d]Department of Biological Sciences, Florida Atlantic University, Boca Raton, FL 33431

† Electronic Supplementary Information (ESI) available: [includes 2D NMR spectra; ESI-MS] See DOI: 10.1039/b000000x/

1. U. S. Schubert, A. Winter and G. R. Newkome, *Terpyridine-based Materials - For Catalytic, Optoelectronic, and Life Science Applications*, Wiley-VCH, Weinheim, Germany, 2011.
2. R. Chakrabarty, P. S. Mukherjee and P. J. Stang, *Chem. Rev.*, 2011, **111**, 6810-6918.
3. B. H. Northrop, H.-B. Yang and P. J. Stang, *Chem. Commun.*, 2008, **45**, 5896-5908.
4. H. Jude, H. Disteldorf, S. Fischer, T. Wedge, A. M. Hawkridge, A. M. Arif, M. F. Hawthorne, D. C. Muddiman and P. J. Stang, *J. Am. Chem. Soc.*, 2005, **127**, 12131-12139.

5. N. Das, P. J. Stang, A. M. Arif and C. F. Campana, *J. Org. Chem.,* 2005, **70**, 10440-10446.
6. J.-L. Wang, X. Li, X. Lu, I.-F. Hsieh, Y. Cao, C. N. Moorefield, C. Wesdemiotis, S. Z. D. Cheng and G. R. Newkome, *J. Am. Chem. Soc.,* 2011, **133**, 11450-11453.
7. A. Schultz, Y. Cao, M. Huang, S. Z. D. Cheng, X. Li, C. N. Moorefield, C. Wesdemiotis and G. R. Newkome, *Dalton Trans.*, 2012, **41**, 11573-11575.
8. X. Lu, X. Li, Y. Cao, A. Schultz, J.-L. Wang, C. N. Moorefield, C. Wesdemiotis, S. Z. D. Cheng and G. R. Newkome, *Angew. Chem. Int. Ed.,* 2013, **52**, 7728 –7731.
9. U. S. Schubert, H. Hofmeier and G. R. Newkome, *Modern Terpyridine Chemistry*, Wiley-VCH, Weinheim, 2006.
10. S.-H. Hwang, C. N. Moorefield, F. R. Fronczek, O. Lukoyanova, L. Echegoyen and G. R. Newkome, *Chem. Commun.*, 2005, 713-715.
11. R. Sarkar, K. Guo, C. N. Moorefield, M. J. Saunders, C. Wesdemiotis and G. R. Newkome, *Angew. Chem. Int. Ed.*, 2014, **53**, 12182-12185.
12. X. Lu, X. Li, J.-L. Wang, C. N. Moorefield, C. Wesdemiotis and G. R. Newkome, *Chem. Commun.*, 2012, 48, 9873-9875.
13. E. C. Constable, C. E. Housecroft, M. Neuburger, S. Schaffner and C. B. Smith, *Dalton Trans.*, 2005, 2259-2267.
14. A. Peuronen, S. Forsblom and M. Lahtinen, *Chem. Commun.*, 2014, **50**, 5469-5472.
15. M. D. Ward, *Chem. Commun*., 2009, 4487-4499.
16. Q. Chen, F. Jiang, D. Yuan, L. Chen, G. Lyu and M. Hong, *Chem. Commun.*, 2013, **49**, 719-721.
17. S. J. Cantrill, M. C. T. Fyfe, A. M. Heiss, J. F. Stoddart, A. J. P. White and D. J. Williams, *Org. Lett.*, 1999, **2**, 61-64.
18. N. Miyaura, T. Yanagi and A. Suzuki, *Syn. Comm.*, 1981, **11**, 513-519.
19. I. Eryazici, P. Wang, C. N. Moorefield, M. Panzer, S. Durmus, C. D. Shreiner and G. R. Newkome, *Dalton Trans.*, 2007, 626-628.
20. J. M. Ludlow III, M. Tominaga, Y. Chujo, A. Schultz, X. Lu, T. Xie, K. Guo, C. N. Moorefield, C. Wesdemiotis and G. R. Newkome, *Dalton Trans.*, 2014, **43**, 9604-9611.
21. A. Schultz, X. Li, C. N. Moorefield, C. Wesdemiotis and G. R. Newkome, *Eur. J. Inorg. Chem.*, 2013, 2492-2497.
22. X. Li, Y.-T. Chan, M. Casiano-Maldonado, J. Yu, G. A. Carri, G. R. Newkome and C. Wesdemiotis, *Anal. Chem.*, 2011, **83**, 6667-6674.
23. J. Thiel, D. Yang, M. N. Rosnes, X. Liu, C. Yvon, S. E. Kelly, Y.-F. Song, D.-L. Long and L. Cronin, *Angew. Chem. Int. Ed.*, 2011, **50**, 8871-8875.
24. M. T. Bowers, P. R. Kemper, G. v. Helden and P. A. M. v. Koppen, *Science* 1993, **260**, 1446-1451.
25. E. R. Brocker, S. E. Anderson, B. H. Northrop, P. J. Stang and M. T. Bowers, *J. Am. Chem. Soc.*, 2010, **132**, 13486-13494.
26. Y.-T. Chan, X. Li, J. Yu, G. A. Carri, C. N. Moorefield, G. R. Newkome and C. Wesdemiotis, *J. Am. Chem. Soc.*, 2011, **133**, 11967-11976.
27. J. Ujma, M. D. Cecco, O. Chepelin, H. Levene, C. Moffat, S. J. Pike, P. J. Lusby and P. E. Barran, *Chem. Commun.*, 2012, **48**, 4423 – 4425.
28. S. Tsuzuki, K. Honda, T. Uchimaru, M. Mikami and K. Tanabe, *J. Am. Chem. Soc.*, 2001, **124**, 104-112.
29. E. C. Constable, *Chem. Soc. Rev.*, 2007, **36**, 246-253.
30. S. Mecozzi and J. J. Rebek, *Chem. Eur. J.*, 1998, **4**, 1016-1022.
31. R. Custelcean, *Chem. Soc. Rev.*, 2014, **43**, 1813-1824.

TOC Graphic

Directed flexibility: self-assembly of a supramolecular tetrahedron

James M. Ludlow III, Tingzheng Xie, Zaihong Guo, Kai Guo, Mary Jane Saunders, Charles N. Moorefield, Chrys Wesdemiotis, and George R. Newkome

Self-assembly of 4 terpyridine-modified, flexible crown ether ligands with 12 Zn^{2+} ions results in high yield tetrahedron construction.